Molecular dissection of water and glycerol permeability of the aquaglyceroporin from *Plasmodium falciparum* by mutational analysis

Eric Beitz*†, Slavica Pavlovic-Djuranovic*, Masato Yasui‡, Peter Agre‡, and Joachim E. Schultz*

*Department of Pharmaceutical Biochemistry, University of Tübingen, Morgenstelle 8, D-72076 Tübingen, Germany; and ‡Departments of Biological Chemistry and Medicine, Johns Hopkins University School of Medicine, 725 North Wolfe Street, Baltimore, MD 21205

Contributed by Peter Agre, December 8, 2003

The selectivity of aquaporins for water and solutes is determined by pore diameter. Paradoxically, the wider pores of glycerol facilitators restrict water passage by an unknown mechanism. Earlier we characterized an aquaglyceroporin from *Plasmodium falciparum* with high permeability for both glycerol and water. We use point mutations to demonstrate that amino acids directly lining the pore are not responsible for the excellent water permeability of the *Plasmodium* aquaglyceroporin but affect permeability of pentitols. Within a conserved WET triad in the extracellular C-loop we identified a *Plasmodium* aquaglyceroporin-specific glutamate (E125) located in proximity to a conserved arginine (R196) at the pore mouth. Mutation of E125 to serine largely abolished water permeability. Concomitantly, the activation energy for water permeation was increased by 4 kcal/mol. Mutation of the adjacent tryptophan to cysteine led to irreversible inhibition of water passage by Hg^{2+}. This unequivocally proves the proximity of the couple W124/E125 close to the pore mouth. We conclude that in the *Plasmodium* aquaglyceroporin the electrostatic environment at the extracellular pore entry regulates water permeability.

A functional divide separates the two major branches of the aquaporin family into water specific channels (orthodox aquaporins) and solute facilitators with restricted water permeability [aquaglyceroporins; reviewed by Borgnia *et al.* (1)]. Prototypes of either group, mammalian aquaporin (AQP1) (2–4) and *Escherichia coli* glycerol facilitator (GlpF) (5, 6) have been structurally resolved with high resolution and shown to be surprisingly similar (7). The carbon backbone of AQP1 and GlpF can be superimposed with minor deviations. Both pore layouts are characterized by a ladder of evenly spaced main chain carbonyl oxygens in ≈3.2-Å steps in an otherwise hydrophobic environment (positions 66–68 and 189–191 in Fig. 1*B*). The oxygens funnel water or solute molecules through the pore via hydrogen bonding. The ladder is interrupted in the center of the channel by amide nitrogens from two invariant asparagines [N70(68) and N193(203) in Fig. 1*B*; the prototypical GlpF sequence is used as a reference throughout and the respective GlpF amino acids and positions are added in parenthesis as descriptors whenever an amino acid aquaglyceroporin from *Plasmodium falciparum* (PfAQP) is mentioned]. The pore center is separated from the carbonyl ladder by an ≈5.5-Å wide hydrophobic ring on either side. Further, both pore types share a positively charged arginine in juxtaposition to two aromatic residues at the extracellular pore entry [R196(206), W50(48), and F190(200)] in Fig. 1*B*).

The water specificity of orthodox aquaporins is rationalized by a constriction of ≈2.8 Å in the arginine/aromatic region, which perfectly matches the size of a water molecule and excludes the more protuberant glycerol (4). Aquaglyceroporins have pores of ≈3.5 Å to accommodate the passage of glycerol and other uncharged solutes but paradoxically impede water permeation (6). Explanations are based on the crystal structures and molecular dynamics simulations. According to de Groot and Grubmüller (8), the hydrophobic ring between the outer carbonyl ladder [G189(199), F190(200), and A191(201) in Fig. 1*B*) and the central asparagines [N70(68) and N193(203)] determines the rate-limiting free-energy barrier for water molecules. Others argue that the hydrophilicity of the arginine/aromatic region [W50(48), F190(200), and R196(206) in Fig. 1*B*] regulates the permeability for water (4, 9, 10). In orthodox aquaporins, one of the aromatic residues is a histidine which together with arginine renders more than half of the pore brim polar, whereas in aquaglyceroporins the phenyl- or indolring of the aromatic amino acids create a considerably more hydrophobic pore vestibule. The exclusion of protons and ions is thought to be caused by the central asparagines (9, 11). Here, the passing chain of water is reoriented such that the network of hydrogen bonds between the file of water molecules is disrupted preventing protons from using the water string as a "proton-wire." Others view the arginine residue at the pore mouth as the proton gatekeeper by repelling positive ions (8). In summary, discussions about the pore filters are controversial and biochemical evidence is scarce.

Recently, we identified a single aquaglyceroporin gene, PfAQP, in the malaria parasite *Plasmodium falciparum* (12). Sequence comparisons showed a close relationship with *E. coli* GlpF. In swelling assays, we found that PfAQP is permeated at high rates by both water and glycerol, and thus represents a rare example of an unbiased bifunctional water/glycerol pore. The contrast between structural similarity and functional dissimilarity of PfAQP and GlpF is the more intriguing because PfAQP contains a pair of amino acids [P223(236)/L224(237)] in transmembrane span 6 typical for glycerol pores. Furthermore, this pair has been implicated by mutagenesis to be essential for glycerol permeability and forestall water passage (13). However, PfAQP passes both glycerol and water. Therefore, we used PfAQP to identify amino acid positions that account for its exceptional water permeability.

We show that the negative charge of glutamate 125(S136), which is located in the extracellular C-loop, interacts with the pore entry arginine 196(206) and thus specifically enables high water passage in PfAQP. We conclude that this arginine is critical for modulation of water permeation through aquaglyceroporins.

Materials and Methods

Sequence Alignments and 3D Model of PfAQP. Structure-based protein alignments were calculated by using the CLUSTAL method with the PAM250 matrix. Alignments and topology plots were generated by using the TEXSHADE and TEXTOPO programs (14, 15). For a structural model of PfAQP aquaglyceroporin, the alignment with GlpF was manually adjusted. The PfAQP se-

Abbreviations: AQP, aquaporin; PfAQP, aquaglyceroporin from *Plasmodium falciparum*; GlpF, glycerol facilitator from *Escherichia coli*.

†To whom correspondence should be addressed. E-mail: eric.beitz@uni-tuebingen.de.

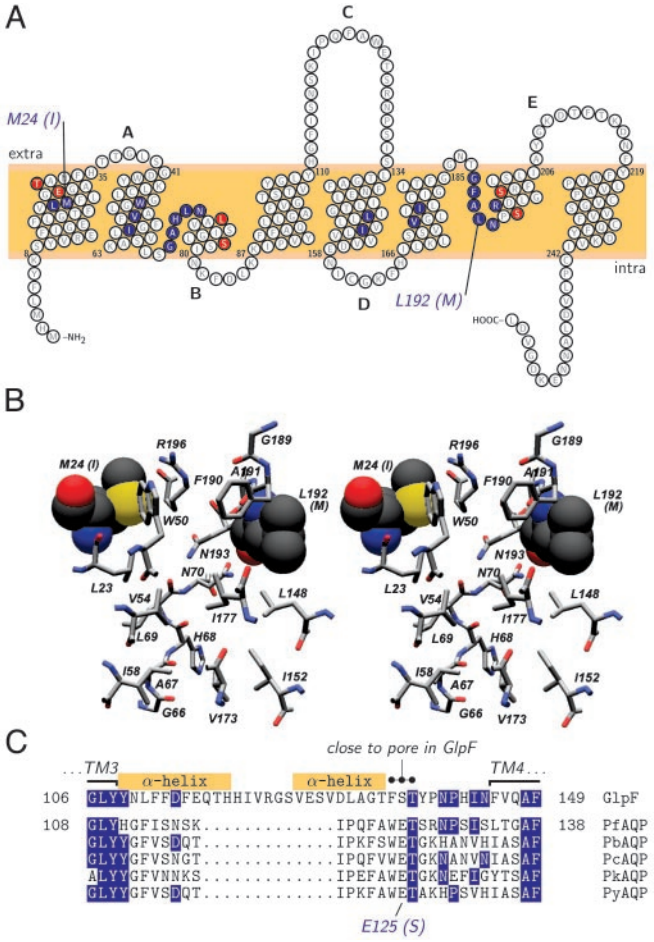

Fig. 1. Sequence and structure comparisons of the aquaglyceroporins of *Plasmodium* and *E. coli*. (*A*) Topology prediction for PfAQP with the pore forming residues shaded blue. Compared to GlpF, only two residues differ in PfAQP within the selective part of the pore, namely M24(I22) and L192(M202). Red-shaded residues indicate six further sequence differences between PfAQP and GlpF in the immediate pore vicinity. Intra- and extracellular loops are labeled alphabetically. (*B*) Stereoview of the pore-lining amino acids (see blue-shaded residues in *A*) as predicted for PfAQP from a sequence projection on the GlpF structure. The two differences in this area [M24(I22) and L192(M202)] are drawn in space filling mode. Bars on the right indicate the proposed filter regions of the aquaporins, i.e., the upper aromatic/arginine filter [W50(48), F190(200), and R196(206)] and the two asparagines in the pore center [N70(68) and N193(203)]. The color scheme follows convention with carbon in gray, nitrogen in blue, oxygen in red, and sulfur in yellow shading. (*C*) Alignment of C-loops from GlpF and aquaglyceroporins from *P. falciparum* (PfAQP), *P. berghei* (PbAQP), *P. chabaudi* (PcAQP), *P. knowlesi* (PkAQP), and *P. yoelii* (PyAQP). Matches between GlpF and the *Plasmodium* aquaglyceroporins are shaded in blue. The superscript dots mark the conserved amino acid triad, which is fixed at the pore entry in GlpF. The *Plasmodium*-specific E125(S136) is highlighted below. Boxes denote the helical regions in the C-loop of GlpF.

quence was then projected onto the 2.2-Å GlpF crystal structure (PDB ID code 1FX8) by using SWISSPDBVIEWER (16). The implemented threading routines were used to minimize the free energy. The termini and connecting loops were not taken into account because of low sequence similarities and substantial length variations.

Cloning and Expression of PfAQP Wild-Type and Point Mutants, Rat AQP1, Rat AQP3, and *E. coli* GlpF. PfAQP and AQP1/AQP3 clones have been described (12). *E. coli* GlpF was amplified from genomic DNA (strain XL1 Blue, Stratagene). Point mutations were introduced by PCR using primers containing the respective nucleotide changes (a list of primers is available upon request). For cloning, nearby endogenous restriction sites were used. In the absence of a suitable restriction site, one was generated by the introduction of silent mutations. Chimeric proteins (loop C exchanges) were also generated by PCR using primers with a common 5′-restriction site. For cRNA synthesis the constructs were subcloned into pOG1 and pOG2, respectively. These vectors are based on pBSTA with the addition of the 5′- and 3′-untranslated regions of the β-globin gene of *Xenopus laevis* around the multiple cloning site. The mMessage mMachine T7 transcription kit (Ambion) was used to produce capped cRNA after linearization with *Not*I. *X. laevis* oocytes of stages V and VI were defolliculated by collagenase A treatment (Roche Molecular Biochemicals) and were injected with 5 ng of cRNA in 50 nl of water. The oocytes were incubated in ND96 buffer (96 mM NaCl/2 mM KCl/1.8 mM $CaCl_2$/1 mM $MgCl_2$/5 mM Hepes, pH 7.4) at 15°C for 3–4 days. Controls received injections of 50 nl of water.

Oocyte Swelling Assays. The assays were carried out as published (12). Briefly, oocytes were transferred either into 1:3 diluted ND96 buffer (140 mOsm/kg gradient) or into isosmotic ND96 in which 65 mM NaCl were replaced by a test solute, e.g., glycerol or xylitol (130 mM chemical gradient). The resulting swelling of the oocytes caused by the influx of water or solute plus water was video monitored. We have reported that, when measuring solute swelling rates, an additional water pathway is needed to allow an unhindered secondary influx of water (12). Therefore, we coinjected oocytes used for solute swelling assays 1:1 with rat AQP1 cRNA. A mercury-insensitive mutant AQP1 C190S was coinjected when the mercury inhibition of PfAQP mutants was assayed. The osmotic water permeability (P_f, in μm/s) was calculated by the equation: $P_f = V_0 \cdot d(V/V_0)/dt/[S \cdot V_W \cdot (\mathrm{osm_{in}} - \mathrm{osm_{out}})]$, with $V = 9 \times 10^{-4}$ cm^3 (initial oocyte volume), $d(V/V_0)/dt$ (relative volume increase in s^{-1}), $S = 0.045$ cm^2 (oocyte surface area), $V_W = 18$ cm^3/mol (molecular water volume), and $\mathrm{osm_{in}} - \mathrm{osm_{out}}$ (osmotic gradient). For a direct comparison of water and solute permeability, the initial swelling rates $[d(V/V_0)/dt]$ were plotted in the graphs. All data are shown with their SEM. Student's *t* test was used to evaluate significance.

Western Blot Analysis. An affinity-purified rabbit polyclonal antiserum against the C-terminal of PfAQP was used (12). Oocytes were lysed in hypotonic phosphate buffer, and the membranes were collected by centrifugation. Membrane proteins equivalent to one oocyte were separated by SDS/PAGE, transferred to poly(vinylidene difluoride) membranes (Macherey & Nagel), probed with the anti-PfAQP antiserum (1:2,000), and detected with horseradish peroxidase-labeled goat anti-rabbit antiserum (Dianova, Hamburg, Germany) by using the ECL Plus system (Amersham Biosciences).

Results

Prediction of Differences in the Pore Lining of PfAQP and GlpF. The facilitated passage of water or solute molecules through aquaporins certainly is affected most by those amino acids that shape the membrane conduit. Hence, we started with a bioinformatics approach to predict pore-lining residues in PfAQP. As a basis we used the crystal structure of GlpF which has 50% overall similarity and 60% similarity in the transmembrane regions with PfAQP. A projection of the PfAQP sequence on the GlpF structure showed that only two amino acids differ between PfAQP and GlpF in the supposedly selective part between the extracellular arginine/aromatic pore edge and its center marked by two asparagines (Fig. 1*B*). The substitutions, M24(I22) and L192(M202), are conservative from a chemical point of view. However, in a channel of ≈3.5-Å diameter, the volume differ-

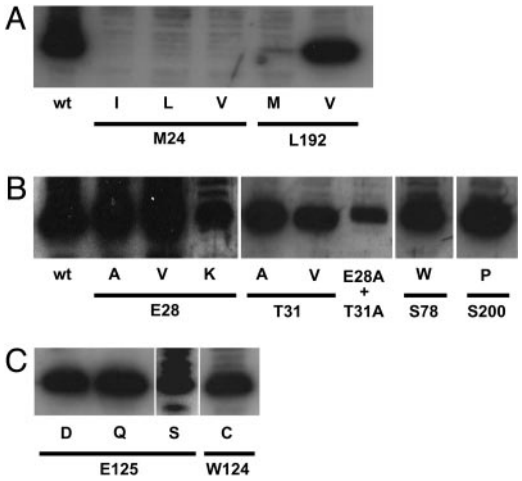

Fig. 2. Expression of PfAQP constructs by Western blotting with *Xenopus* oocyte membranes and an antiserum specific to the C terminus of PfAQP. (*A*) Mutations in the pore lining. (*B*) Mutations in the pore vicinity. (*C*) Mutations in the C-loop. Band broadening and multiple bands may be caused by incomplete secondary modifications and/or unspecific labeling.

ences of the side chains could well modify the pore properties as evident when viewed in a structural context (Fig. 1*B*). The contribution of M24(I22) to the pore lining is restricted to a small fraction of the sulfur atom surface, whereas the side chain of L192(M202) represents a major part of the inner wall of the channel, providing about one-quarter of the hydrophobic ring surface between the outer carbonyl ladder and the two central asparagines.

Characterization of PfAQP M24(I22) and L192(M202) Point Mutants. M24 was conservatively replaced by I, L, and V, and L192(M202) was conservatively replaced by either M or V. Mutant cRNA was injected into *X. laevis* oocytes and protein expression was monitored by Western blotting with an antibody specific to the C terminus of PfAQP (Fig. 2*A*). None of the three M24(I22) point mutants was expressed in the oocytes. Mutant L192M was barely expressed, whereas the L192V construct was present at PfAQP wild-type levels.

The permeability for water and solutes was measured by oocyte swelling in diluted medium (140 mOsm/kg gradient) and in isosmotic medium containing the solute as a partial replacement of NaCl (130 mM gradient). Confirming the Western blot analysis injection of M24(I22)s, mutant cRNAs did not affect oocyte permeability (data not shown). We assume that the proteins were misfolded and degraded. Hence, beyond the notion of the structural importance of M24(I22), we could not determine whether it directly contributes to pore permeability. The L192M mutant was poorly expressed, and increased water and glycerol permeability was expressed only moderately compared to control injected oocytes (Fig. 3*A*). However, the ratio of water vs. glycerol permeability was significantly changed in comparison to the wild-type control ($P < 0.05$). Nevertheless, the high permeability of the L192V mutant for both water and glycerol indicated that L192(M202) probably does contribute little to discriminate between water and glycerol conductance in PfAQP.

An interesting observation is that PfAQP and GlpF allow passage of pentitols such as xylitol, D-arabitol, and ribitol at substantially different rates (6, 12). Surely, the speed of membrane passage depends on the stereochemistry of the polyol and the respective inner pore structure. The preferred permeability sequence of GlpF (ribitol ≫ xylitol ≫ D-arabitol) is opposite to that of PfAQP (xylitol > D-arabitol ≫ ribitol, Fig. 3*B*). The

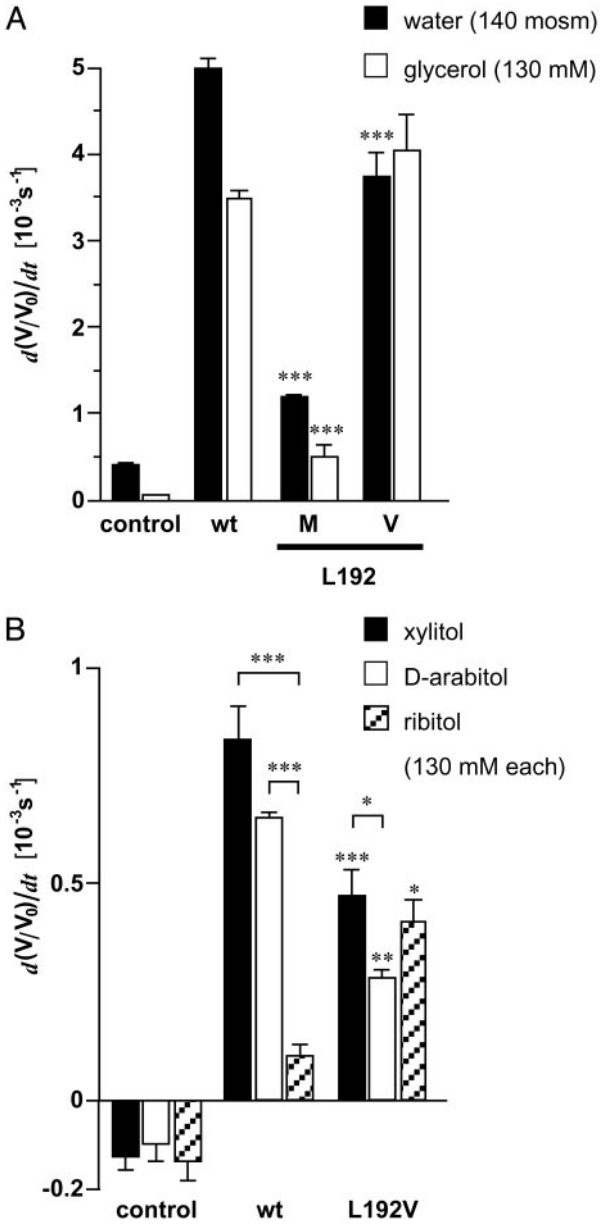

Fig. 3. Swelling of oocytes expressing PfAQP constructs with mutations in the pore lining. (*A*) Swelling rates for water and glycerol ($n = 4–6$). (*B*) Permeability of pentitols through PfAQP and the L192V mutant ($n = 3–5$). Asterisks above the error bars indicate significant differences in the flux rates of the same solute between wild-type and mutant PfAQP. Asterisks above brackets indicate significant differences in the flux rates of different solutes through the same channel protein (*, $P < 0.05$; **, $P < 0.02$; ***, $P < 0.01$).

PfAQP L192V mutant significantly decreased the permeability for xylitol ($P < 0.01$) and D-arabitol ($P < 0.02$) and raised that of ribitol 3-fold ($P < 0.05$; Fig. 3*B*). In agreement with the reduction of water permeability by L192M, this assigns this amino acid a definitive, albeit possibly minor, role in controlling PfAQP solute permeability.

Mutations in the Vicinity of the Pore. Because amino acid differences making up the pore lining did not account for the high water permeability of PfAQP, we looked at the structure of PfAQP and GlpF in the immediate pore vicinity. A total of six nonconservative differences are located in the first transmembrane domain and the hydrophobic half helices of loops B and

BIOCHEMISTRY

Table 1. Swelling rates of PfAQP constructs with mutations in the second sphere around the pore

Mutation	Location	Water, $d(V/V_0)dt$ [10^{-3} s^{-1}]	Glycerol, $d(V/V_0)dt$ [10^{-3} s^{-1}]	Water/glycerol
None (WT)		5.00 ± 0.24	3.49 ± 0.19	1.43
E28V	TM1	3.77 ± 0.29	2.25 ± 0.53	1.68
E28K		3.19 ± 0.25	2.96 ± 0.23	1.08*
E28A		2.93 ± 0.27	3.51 ± 0.23	0.84*
T31V	TM1	3.27 ± 0.31	3.30 ± 0.56	0.99*
T31A		2.80 ± 0.37	2.84 ± 0.36	0.99†
E28A + T31A		2.79 ± 0.36	2.30 ± 0.32	1.21
S78W	Loop B	4.69 ± 0.58	3.48 ± 0.44	1.35
S200P	Loop E	4.49 ± 0.38	3.72 ± 0.56	1.21

TM, transmembrane. Boldface indicates mutations to the residue that is present in GlpF ($n = 4–8$). *, significantly different from wild-type control ($P < 0.05$); †, $P = 0.067$.

E. These are E28(V26), T31(V29), L71(P69), S78(W76), S195(A205), and S200(P210) (marked red in Fig. 1*A*). L71(P60) and S195(A205) in PfAQP convert the two central NPA motifs to NLA and NPS, respectively. As reported earlier, these differences do not affect pore permeability (12). Therefore, we tested whether the remaining four candidate residues are responsible for the water permeability of PfAQP. All mutants were well expressed in the oocytes (Fig. 2*B*) and water and glycerol permeabilities were assessed (Table 1). To evaluate pore selectivity we calculated the ratio of water vs. glycerol fluxes. The reduced glycerol permeability observed in E28K, charge inversion, E28A, smaller side chain, and T31V hydrophobicity increase, was statistically significant, and the effect T31A was statistically borderline (Table 1). All other mutants did not significantly alter the ratio of water/glycerol permeability.

In summary then, L192(M202), E28(V26), and T31(V29) participate in regulation of solute fluxes; however, these data do not explain the high water permeability in this aquaglyercoporin.

Sequence Diversity in Loop C. The extracellular connecting loop C is a characteristic discriminator between orthodox aquaporins and aquaglyceroporins because it differs in length by 15 aa (7). Structurally, the C-loop dips into the outer pore vestibule and is fixed via hydrogen bonds close to the arginine of the upper filter region (4, 6). Furthermore, in aquaglyceroporins, a triad of amino acids containing an invariable threonine is highly conserved throughout evolution (FST in *E. coli*, FAT in mammals) which is located close to the pore in GlpF (6). In contrast to other aquaglyceroporins, in PfAQP, the C-loop is more akin to orthodox aquaporins (23 vs. 21 amino acids), yet without any sequence similarity. By the same token, the C-loop of GlpF is unlike that of PfAQP (Fig. 1*C*). In GlpF, the C-loop folds as two α-helices. Because in PfAQP 13 amino acids are missing in this region, the structure must look different. This prevented us from predicting the fold of the PfAQP C-loop. Only within the C-terminal eight positions of the C-loop four residues match including an invariable threonine. Due to several recent *Plasmodium* genome projects (*Plasmodium berghei*, *Plasmodium chabaudi*, *Plasmodium knowlesi*, *Plasmodium yoelii*) we could compare homologous aquaglyceroporin sequences. As in *P. falciparum*, these genomes so far contain only a single aquaglyceroporin gene. The similarity of these species variants to PfAQP is >80%. Notably, the highly conserved triad FST of the C-loop is uniformly WET in the *Plasmodium* aquaglyceroporins (Fig. 1*C*) strongly implying that, in all *Plasmodium* aquaglyceroporins, a negatively charged glutamate is in direct proximity to the positive pore arginine where conventional aquaglyceroporins have either an uncharged serine or alanine.

PfAQP E125(S136) Is Responsible for the High Water Permeability. In a first survey experiment, loop C of PfAQP (position 111–133, Fig. 1*C*) was swapped with that of GlpF (position 109–144). However, this chimera was not expressed in the oocyte and could not be examined (data not shown). Next, E125(S136) in PfAQP was mutated to D, Q, and S. Western blot analysis showed expression of these constructs (Fig. 2*C*). All E125(S136) point mutants passed glycerol at rates of at least 66% of PfAQP wild-type. Statistically, these differences were not significant. However, the mutations dramatically affected water permeability. When an aspartate or glutamine was used as a substitute for E125(S136), water permeability was 55% and 42% of wild-type, respectively. The mutation of E125(S136) to serine, i.e., the residue present in GlpF, reduced water permeability almost completely (Fig. 4*A*). Thus, the structural and functional properties that prevail in GlpF, seem to be matched in this mutant.

To further prove that the WET triad of the PfAQP C-loop is closely connected with the pore function, we mutated the tryptophan to cysteine (W124C). The cysteine should provide a binding site for a mercury ion, which should severely interfere with channel permeability provided the above interpretation is correct. Wild-type PfAQP is not inhibited by mercury, although six cysteine residues are present (12). Obviously, these cysteines are not connected to function. PfAQP W124C was expressed in *Xenopus* oocytes (Fig. 2*C*) and passed water and glycerol at about one-third the rate of the wild-type PfAQP, perhaps indicating a region critical for channel function (Fig. 4*B*). Preincubation of oocytes for 5 min with 0.3 mM Hg^{2+} fully blocked water and glycerol permeability (Fig. 4*B*). Recovery by the addition of 3 mM 2-mercaptoethanol was only marginal. This proves unequivocally that W124(F135) and E125(S136) are structurally and functionally coupled to water and glycerol passage.

Finally, the effect of the E125S mutation on the Arrhenius activation energy was measured in comparison to the wild-type channel and control oocytes (Fig. 5). Nonfacilitated water permeation through the oocyte membrane required an activation energy of 10.5 kcal/mol. This value is three times higher than that for the facilitated water diffusion through PfAQP (3.5 kcal/mol). The replacement of E125(S136) by serine increased the energy which is needed for water permeation by 4 kcal/mol to 7.5 kcal/mol.

Discussion

The striking sequence similarity of PfAQP and GlpF of *E. coli* suggests that, in the malaria parasite, a bifunctional solute channel of bacterial origin has evolved. Combining two physiologically distinct functions in a single channel is in line with the principle of minimizing the number of membrane proteins to reduce antigenic structures on the cell surface. This seems to be a common theme in *Plasmodium* as seen by the restricted repertoire of predicted membrane transporters in the parasite genome (17). The genome annotation forecasts that the PfAQP represents one of a total of six members of the major facilitator superfamily for organic nutrients. It has to be kept in mind, however, that ≈60% of all predicted proteins in *Plasmodium* are not as yet functionally categorized; i.e., more facilitators of unusual structure might be identified in the future.

Apart from this evolutionary aspect, PfAQP proved to be a valuable model pore for studying water permeability in aquaglyceroporins because of its extraordinary water permeability. Further to this point, high sequence similarity to GlpF reduced the set of candidate amino acid residues to a testable number. Our initial PfAQP mutants dealt with amino acid substitutions in the pore lining or in the sphere directly around the pore. These mutations either had only limited effects on the ratio of water

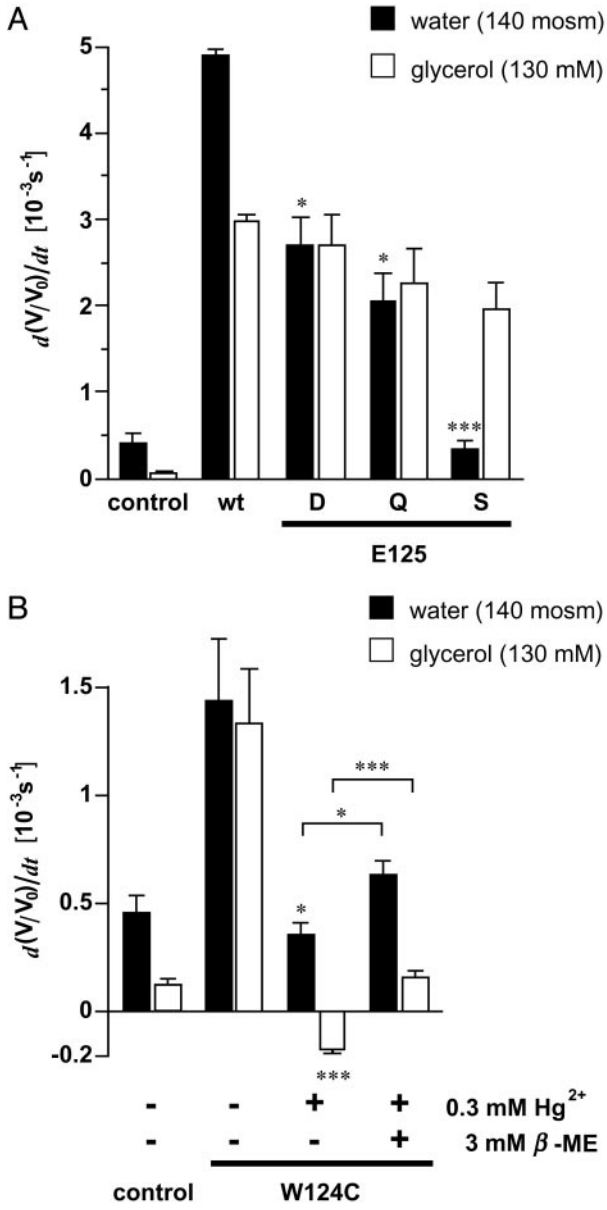

Fig. 4. Swelling rates of oocytes expressing PfAQP with C-loop mutations. (*A*) Water and glycerol swelling rates ($n = 5–8$ and 3–5 for water and glycerol, respectively). Glycerol permeability was not significantly different. Asterisks above the error bars indicate significant differences in the water permeability between wild-type and mutant PfAQP. (*B*) Effect of Hg^{2+} on water and glycerol permeation of PfAQP W124C. Swelling rates of oocytes were determined before and after 5 min incubation in ND96 medium with 0.3 mM Hg^{2+}. Furthermore, swelling rates of oocytes are shown that were held in ND96 with 3 mM 2-mercaptoethanol for >10 min after the mercury inhibition ($n = 3–6$). Asterisks above the error bars indicate significant differences in the water and glycerol permeabilty before and after mercury treatment. Asterisks above brackets indicate significance levels of the recovery of water and glycerol permeability after incubation in 2-mercaptoethanol (*, $P < 0.05$; **, $P < 0.02$; ***, $P < 0.01$).

and glycerol permeability or were not functional because of expression problems. This "all-or-nothing" effect might be explained by the rigidity of the aquaporin core structure that is required to stabilize a channel with a diameter of 3.5 Å over a length of 25 Å (18). Some changes may be compatible with the structure and, hence, function, whereas others obviously cannot be reconciled with the structural requirements. Those mutations

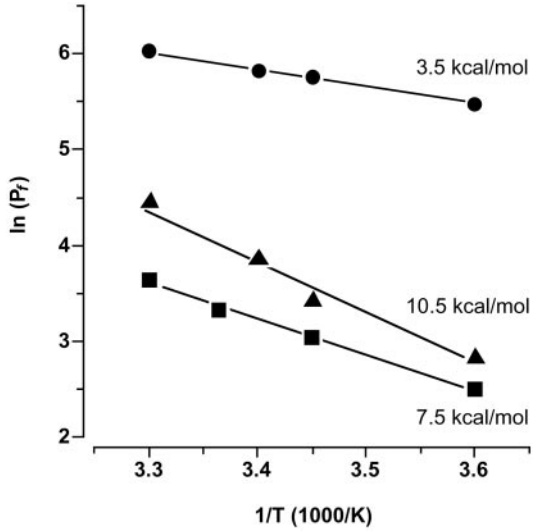

Fig. 5. Arrhenius plot of the water permeability (P_f) through PfAQP wild-type (circles), PfAQP E125S (squares), and control oocyte membranes (triangles). Plotted are logarithms of the P_f values against reciprocals of the temperature at which the measurements were carried out (4–30°C). Activation energies were calculated from the slopes of the linear fits ($n = 5$).

in this section that worked clearly demonstrate that the discrimination between water and glycerol permeability does not occur inside the channel itself.

The outer pore mouth is dominated by a positive arginine embedded in an aromatic environment. Crystallography and ensuing molecular dynamics simulations showed that in GlpF the space between the two aromatic residues (W48 and F200 in GlpF) is barely occupied by water molecules (6, 9). When W48 in GlpF was replaced by phenylalanine and F200 by a threonine to render the area wider and more hydrophilic, water occupancy was enhanced, and the water permeability of such a GlpF mutant was increased (9). This very principle of adding polarity to the aromatic/arginine mouth region is realized in several aquaglyceroporins with limited water permeability, e.g., in the mammalian AQP3, which carries a tyrosine instead of a phenylalanine. By comparison, orthodox aquaporins possess a histidine as one of the aromatic residues (4, 10). The highly water permeable PfAQP has tryptophan [W50(48)] and phenylalanine [F190(200)] in this area, as does the poorly water permeable GlpF. Therefore, it must be concluded that a new mechanism to facilitate water passage has evolved in the malaria aquaglyceroporin.

Three lines of evidence suggest that E125(S136) in the extracellular C-loop is critically responsible for the high water permeability of PfAQP. Firstly, mutation of the glutamate to serine greatly reduces water permeability. Secondly, E125(S136) is situated close to the pore mouth as shown by the gain of mercury sensitivity of a mutant where the adjacent tryptophan [W124(F135)] is changed to cysteine. Thirdly, considering the differences in the Arrhenius activation energies we reason that in wild-type PfAQP the positive charge of R196(206) is largely neutralized or even spatially fixed by E125(S136). Fersht *et al.* have determined the contribution of different types of hydrogen bonds to the binding energy between an enzyme and its substrate by specifically deleting single hydrogen bonding sites in the tyrosyl–tRNA synthetase (19). They concluded that hydrogen bonds between two polar but uncharged partners stabilize the interaction by 0.5–1.5 kcal/mol whereas ≈3 kcal/mol are gained when one of the hydrogen-bond partners is charged. The difference in activation energies of the E125S mutant and wild-type

PfAQP corresponded well with these data. Thus, we conclude that in wild-type PfAQP the strength of hydrogen bonds of passing water molecules with R196(206) is reduced because of charge compensation by E125(S136). This might allow for single water molecules to more rapidly file through the pore. Apparently, changes in the electrostatic environment at the pore mouth affect this hydrogen bonding process. This is evident from the increase of the activation energy in the PfAQP E125S mutant from 3.5 kcal/mol (PfAQP wild-type) to 7.5 kcal/mol and, consequently, 10-fold reduction in water permeability. These numbers perfectly agree with the activation energies of the orthodox aquaporin Z from *E. coli* and GlpF of 3 kcal/mol and 7 kcal/mol, respectively (20). In the reported liposome system the water permeability similarly differed by one order of magnitude. However, resolving the hydrogen-bond network of bulk water into a single file of molecules for pore passage is possible without a charged arginine directly at the pore mouth. This solution has been accomplished in an aquaporin family from plants, tonoplast intrinsic proteins, TIP (21). Here, the pore mouth is designed without any charged residue. The pores of this family contain a valine instead of the arginine and are water selective with P_f values $\approx$150 μm·sec^{-1}, an intermediate aquaporin water permeability value. Furthermore, although a repelling positive charge is missing in the pore, TIP channels are also impermeable for ions (21). The extreme in terms of pore layout is reached in entirely hydrophobic carbon nanotubes. According to molecular dynamics simulations, water enters and passes through these channels in single file despite the total lack of polarity (22).

Having identified E125(S136) as critical for water permeability of PfAQP, the question arises whether this channel is still impermeable for protons and other ions although the positive charge of the pore arginine is fully or partially neutralized. We carried out electrophysiological recordings in isosmotic medium by using a voltage stepping protocol at different pH values (23). Thereby an ion conductance of PfAQP was excluded (not shown). Therefore, we propose that the arginine in PfAQP does not operate as a gatekeeper against passage of ions or protons.

Another question would be whether classical aquaglyceroporins could be induced to pass water by introduction of a negative charge in the C-loop. Swapping the C-loops in AQP3 and GlpF with PfAQP led to inactive channels (data not shown). As already seen with the reverse chimera, the loop structures are not readily interchangeable between PfAQP and other aquaglyceroporins. Here, stabilizing interaction sites between the loop and the protein core are probably not compatible leading to misfolding and degradation. Substitution of the central residue of the F(S/A)T triad in AQP3 and GlpF by glutamate or aspartate resulted in barely functional channels but an increase in water permeability could not be established by these modifications (data not shown). We think that, in PfAQP, the highly divergent C-loop sequence is critically involved in the exact positioning of the charge. Probably, the switch from a glycerol facilitator to a bifunctional aquaglyceroporin needs a number of fine adjustments. Evolutionary developments of such an extent are particularly expedited in a dynamic parasite–host relation with an enormous selective pressure. It can be expected that more examples of basic structural and functional conversions will be found in the *Plasmodium* proteome.

We thank A. Schultz for technical assistance and N. Kumar and R. Stroud for critically reading the manuscript. We also thank P. Krippeit-Drews for help with the *Xenopus* frogs. The work was funded by the Deutsche Forschungsgemeinschaft (Be2253/2-1) and grants from the National Institutes of Health.

1. Borgnia, M., Nielsen, S., Engel, A. & Agre, P. (1999) *Annu. Rev. Biochem.* **68,** 425–458.
2. Walz, T., Hirai, T., Murata, K., Heymann, J. B., Mitsuoka, K., Fujiyoshi, Y., Smith, B. L., Agre, P. & Engel, A. (1997) *Nature* **387,** 624–627.
3. Cheng, A., van Hoek, A. N., Yeager, M., Verkman, A. S. & Mitra, A. K. (1997) *Nature* **387,** 627–630.
4. Sui, H., Han, B. G., Lee, J. K., Walian, P. & Jap, B. K. (2001) *Nature* **414,** 872–878.
5. Braun, T., Philippsen, A., Wirtz, S., Borgnia, M. J., Agre, P., Kühlbrandt, W., Engel, A. & Stahlberg, H. (2000) *EMBO Rep.* **1,** 183–189.
6. Fu, D., Libson, A., Miercke, L. J., Weitzman, C., Nollert, P., Krucinski, J. & Stroud, R. M. (2000) *Science* **290,** 481–486.
7. Engel, A., Fujiyoshi, Y. & Agre, P. (2000) *EMBO J.* **19,** 800–806.
8. De Groot, B. L. & Grubmüller, H. (2001) *Science* **294,** 2353–2357.
9. Tajkhorshid, E., Nollert, P., Jensen, M. O., Miercke, L. J., O'Connell, J., Stroud, R. M. & Schulten, K. (2002) *Science* **296,** 525–530.
10. Thomas, D., Bron, P., Ranchy, G., Duchesne, L., Cavalier, A., Rolland, J. P., Raguenes-Nicol, C., Hubert, J. F., Haase, W. & Delamarche, C. (2002) *Biochim. Biophys. Acta* **1555,** 181–186.
11. Murata, K., Mitsuoka, K., Hirai, T., Walz, T., Agre, P., Heymann, J. B., Engel, A. & Fujiyoshi, Y. (2000) *Nature* **407,** 599–605.
12. Hansen, M., Kun, J. F. J., Schultz, J. E. & Beitz, E. (2002) *J. Biol. Chem.* **277,** 4874–4882.
13. Lagree, V., Froger, A., Deschamps, S., Hubert, J. F., Delamarche, C., Bonnec, G., Thomas, D., Gouranton, J. & Pellerin, I. (1999) *J. Biol. Chem.* **274,** 6817–6819.
14. Beitz, E. (2000) *Bioinformatics* **16,** 135–139.
15. Beitz, E. (2000) *Bioinformatics* **16,** 1050–1051.
16. Guex, N. & Peitsch, M. C. (1997) *Electrophoresis* **18,** 2714–2723.
17. Gardner, M. J., Hall, N., Fung, E., White, O., Berriman, M., Hyman, R. W., Carlton, J. M., Pain, A., Nelson, K. E., Bowman, S., *et al.* (2002) *Nature* **419,** 498–511.
18. Jensen, M. O., Park, S., Tajkhorshid, E. & Schulten, K. (2002) *Proc. Natl. Acad. Sci. USA* **99,** 6731–6736.
19. Fersht, A. R., Shi, J. P., Knill-Jones, J., Lowe, D. M., Wilkinson, A. J., Blow, D. M., Brick, P., Carter, P., Waye, M. M. & Winter, G. (1985) *Nature* **314,** 235–238.
20. Borgnia, M. J. & Agre, P. (2001) *Proc. Natl. Acad. Sci. USA* **98,** 2888–2893.
21. Maurel, C., Reizer, J., Schroeder, J. I. & Chrispeels, M. J. (1993) *EMBO J.* **12,** 2241–2247.
22. Hummer, G., Rasaiah, J. C. & Noworyta, J. P. (2001) *Nature* **414,** 188–190.
23. Yasui, M., Hazama, A., Kwon, T. H., Nielsen, S., Guggino, W. B. & Agre, P. (1999) *Nature* **402,** 184–187.